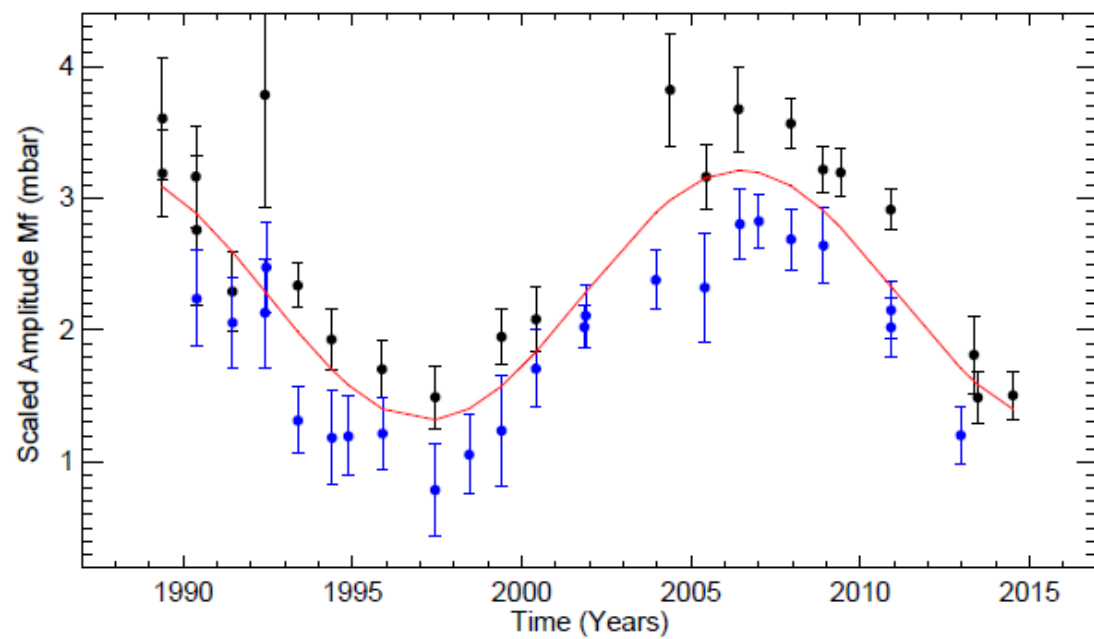
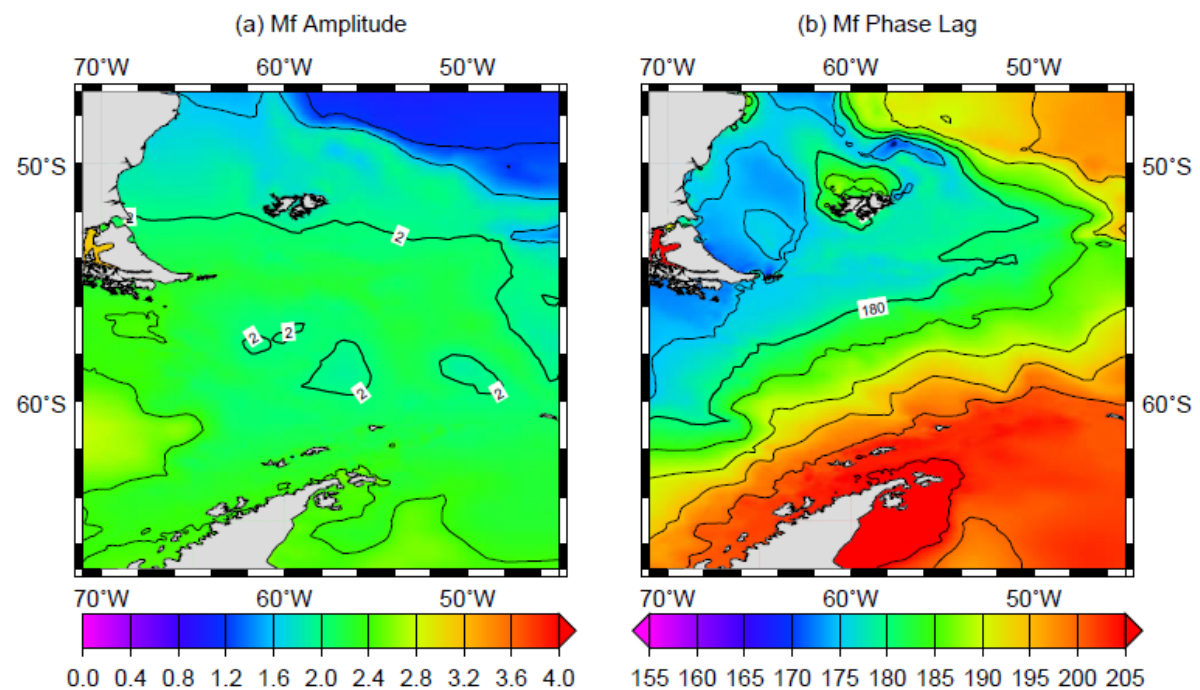


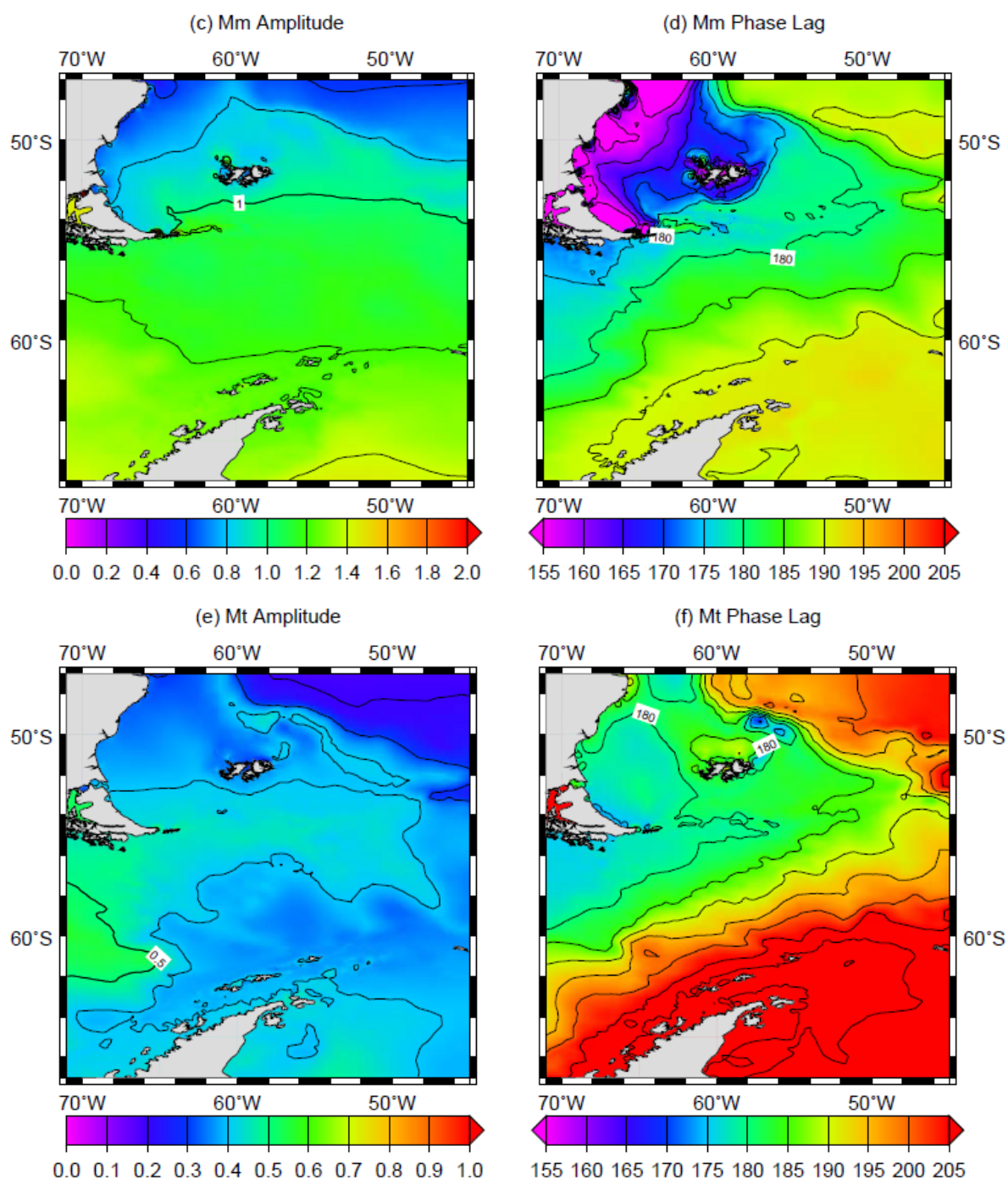
Supplementary Figures



Supplementary Figure 1

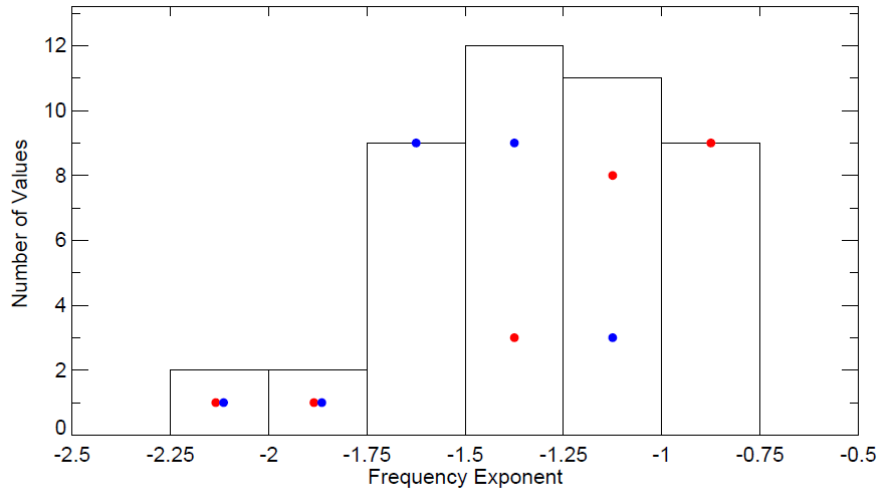
Amplitude for M_f as in Figure 5 (a) but with corrections for latitude assuming an equilibrium-tide dependence (see text).





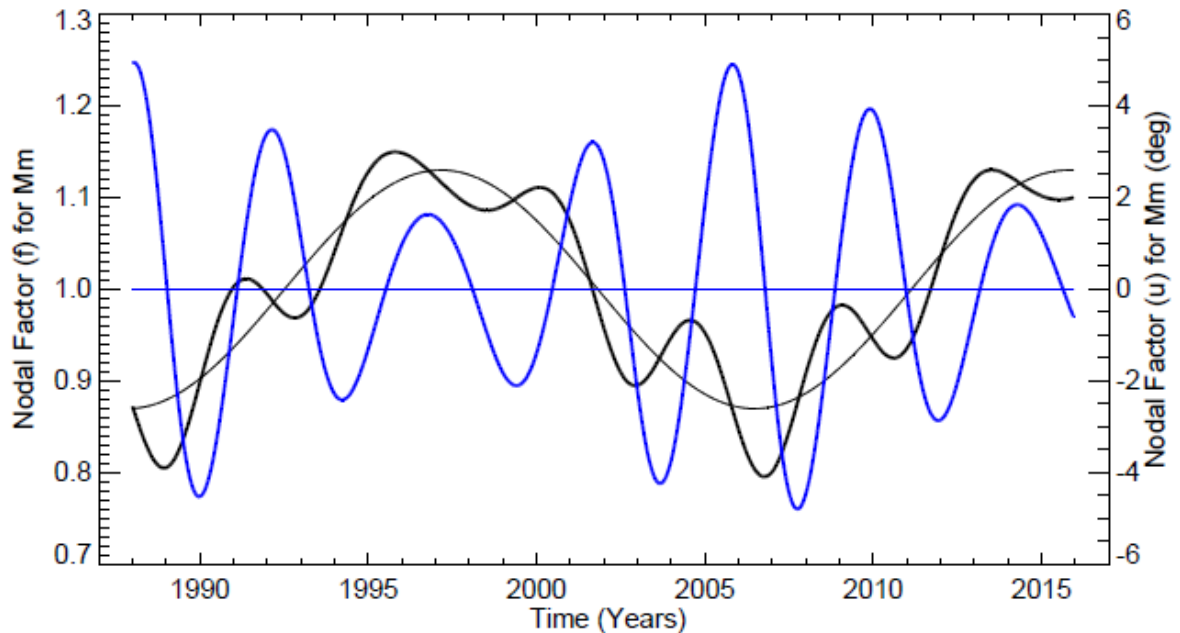
Supplementary Figure 2

(a) Amplitude (cm) and (b) Greenwich phase lag (deg) for Mf as represented in the FES2014 ocean tide model; (c,d) As (a,b) but for Mm; (e,f) As (a,b) but for Mt. Amplitudes contours are every 0.4, 0.2 and 0.1 cm in (a,c,e) respectively, while phase lags are contoured every 5°.



Supplementary Figure 3

A histogram of the exponents ' k ' obtained from fits to the non-tidal power spectra of each of the 45 BPR deployments at Drake Passage, power being parameterised by (frequency^k) over the full range of frequency (0-0.5 cycles per day). $k=0$ would represent white noise, $k=-1$ corresponds to pink or flicker noise. The numbers of south and north deployments (23 and 22 in total respectively) in each bin are shown by the blue and red dots. k can be seen to be on average more negative in the south, which is initially surprising as eddies are more prevalent in the north (Sheen et al., 2014), and would be expected to lead to steeper spectra. However, there are other processes contributing to BP variability (e.g. the Madden-Julian Oscillation, Matthews and Meredith, 2004), and such a north-south difference in ' k ' is in fact consistent with model findings (e.g. Figure 3 of Hughes et al., 2018).



Supplementary Figure 4

The nodal factors f and u for Mm at 58°S as in Figure 10 but including the 2nd-degree sidebands only (i.e. the first 4 and 2 terms in Equation A9 for $f \cos(u)$ and $f \sin(u)$ respectively).